Xin Zhang, Sai Mu, Yang Liu, Jian Luo, Jian Zhang,
Alpha T. N'Diaye, Axel Enders and Peter A. Dowben*

The Electronic Structure Signature of the Spin Cross-Over Transition of [Co(dpzca)$_2$]

https://doi.org/10.1515/zpch-2017-0932
Received January 24, 2017; accepted December 7, 2017

Abstract: The unoccupied electronic structure of the spin crossover molecule cobalt (II) N-(2-pyrazylcarbonyl)-2-pyrazinecarboxamide, [Co(dpzca)$_2$] was investigated, using X-ray absorption spectroscopy (XAS) and compared with magnetometry (SQUID) measurements. The temperature dependence of the XAS and molecular magnetic susceptibility $\chi_m T$ are in general agreement for [Co(dpzca)$_2$], and consistent with density functional theory (DFT). This agreement of magnetic susceptibility and X-ray absorption spectroscopy provides strong evidence that the changes in magnetic moment can be ascribed to changes in electronic structure. Calculations show the choice of Coulomb correlation energy *U* has a profound effect on the electronic structure of the low spin state, but has little influence on the electronic structure of the high spin state. In the temperature dependence of the XAS, there is also evidence of an X-ray induced excited state trapping for [Co(dpzca)$_2$] at 15 K.

Keywords: cobalt (II) N-(2-pyrazylcarbonyl)-2-pyrazinecarboxamide; density functional theory; spin crossover transition; X-ray induced excited state trapping.

1 Introduction

The spin crossover molecule cobalt (II) {N-(2-pyrazylcarbonyl)-2-pyrazinecarboxamide}$_2$, i.e. [Co(dpzca)$_2$], is known to have a hysteretic thermal spin crossover

***Corresponding author: Peter A. Dowben,** Department of Physics and Astronomy, University of Nebraska-Lincoln, Theodore Jorgensen Hall, 855 North 16th Street, Lincoln, NE 68588-0299, USA, Tel.: +402-472-9838, Fax: +402-472-6148, e-mail: pdowben1@unl.edu
Xin Zhang, Sai Mu and Yang Liu: Department of Physics and Astronomy, University of Nebraska-Lincoln, Theodore Jorgensen Hall, 855 North 16th Street, Lincoln, NE 68588-0299, USA
Jian Luo and Jian Zhang: Department of Chemistry, University of Nebraska–Lincoln, Hamilton Hall, Lincoln, NE 68588-0304, USA
Alpha T. N'Diaye: Advanced Light Source, Lawrence Berkeley National Laboratory, Berkeley, CA 94720, USA
Axel Enders: Universität Bayreuth, Physikalisches Institut, Naturwissenschaften I, Universitätsstraße 30, 95447 Bayreuth, Germany

transition from a low spin to high spin state [1–4]. Typical of most spin crossover molecular systems, $[Co(dpzca)_2]$ has a temperature induced spin crossover transition, but also exhibits a pressure induced spin crossover transition [4] that pushes the transition to higher temperatures. What makes this system even more interesting is that $[Co(dpzca)_2]$ can undergo reversible redox reactions [2, 3]. This is important as only a few metal-organic spin crossover molecular systems have been demonstrated to undergo such reactions reversibly.

As a Co^{2+} cation ($3d^7$) spin cross-over system, the low spin state of $[Co(dpzca)_2]$, observed below 160 K, is not zero spin, as is evident in the magnetization studies [1, 3, 4]. The implication is that the low spin state remains a state with finite moment so that the molecule itself is not diamagnetic. This means that this spin crossover transition is a meta-paramagnetic transition from a moment paramagnetic state to a higher moment paramagnetic state, not a transition from a diamagnetic low spin state to a paramagnet high spin state, as is the case for the Fe(II) spin crossover systems which tend to be diamagnetic in the low spin state.

Here we investigate the correlation between the magnetic moment and the electronic structure with a combination of density functional theory and X-ray absorption spectroscopy (XAS). Generally electronic structure changes across the spin crossover transition are a reflection of the changes in the magnetic susceptibility during the spin crossover transition at the critical temperature. Nonetheless, it has recently become evident that electronic structure is not always in 'lock-step' with the magnetization, when determined by a final state spectroscopy like X-ray absorption spectroscopy [5]. With $[Co(dpzca)_2]$, we have a system where structural distortions have a profound effect on the magnetic properties [4] and is yet a system where a Coulomb correlation energy U may play a role in accurately assessing the electronic structure, as has now been seen elsewhere [5].

2 Experimental methods

The $[Co(dpzca)_2]$ was synthesized according to the procedures outlined previously by the Brooker group [2, 3]. A molecular powder was used in the experiments, spread on a vacuum compatible carbon tape. The X-ray absorption spectroscopy (XAS) measurements were performed at the bending magnet beamline 6.3.1 at the advanced light source at Lawrence Berkeley National Laboratory. The photon flux is on the order of 1×10^{11} photons/s/0.1%BW [6]. The sample temperature was stabilized within ±0.1 degrees Kelvin. Positive circularly polarized X-ray radiation was used, with a spectral resolution of $\lambda/\Delta\lambda \approx 2000$. The total electron yield (TEY) mode was used to measure the absorption at the Co $2p_{3/2}$ (the L_{III}) edge and each XAS spectrum took about 150 s to complete, though faster scan speeds

were used for the time dependent soft X-ray induced excited spin state trapping (SOXIESST) studies. The temperature-dependent magnetic properties were measured by superconducting quantum interference device (SQUID) magnetometry using a Quantum Design magnetic property measurement system (MPMS).

3 Theoretical methodology

The first-principles calculations were carried out using projected augmented wave method (PAW) [7], as implemented in the Vienna *ab initio* simulation package (VASP) [8, 9]. Both the high spin (HS) state and low spin (LS) state were obtained to confirm the ground state for [Co(dpzca)$_2$], for each spin state structure. To describe the electronic structure correctly, we used the rotationally invariant generalized gradient approximation (GGA) + U method [10], but with no spin built-in exchange splitting. The GGA was parameterized using the scheme proposed by Perdew et al. [11]. It is evident that the neglect of the spin exchange splitting gives reasonable agreement with more sophisticated DFT + DMFT (density functional theory combined with dynamical mean field theory) methods in determining the HS-LS energy splitting in Fe(phen)$_2$(NCS)$_2$ [12]. We have set the Coulomb correlation energy $U = 5.0$ eV and the exchange energy $J = 0.9$ eV, as is suitable for the localized 3d orbitals on Co atoms. We constructed a tetragonal cell (space group: $I4_1/a$), as seen in Figure 1, and monoclinic unit cell (space group: $P2_1/c$), using the high temperature (high spin state) and low temperature (low spin state) structures of [Co(dpzca)$_2$], respectively, adopted from the experimental crystal structures [3]. A plane-wave energy cutoff of 500 eV and a $6 \times 6 \times 2$ K-point mesh were employed for the total energy and electronic structure calculations. A Gaussian smearing of 0.03 eV was adopted for energy calculations and a smearing of 0.1 eV was used for plotting the density of states (DOS), so as to better compare with experiment. The high spin state and low spin state were stabilized based on high temperature and low temperature molecular structures, respectively, as just mentioned.

4 Results and discussion

4.1 The nonzero moment low spin state

As seen in the experimental SQUID measurements shown in Figure 2, the magnetic moment of the molecules is nonzero below and above the spin crossover

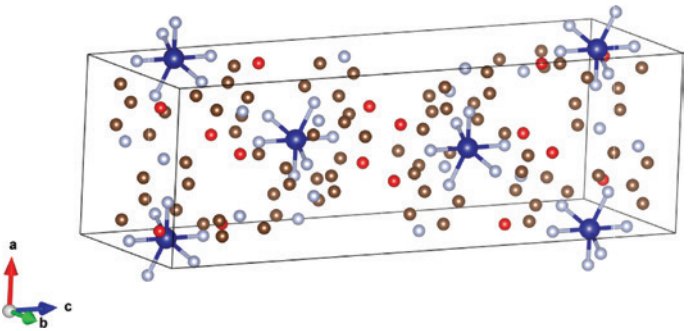

Fig. 1: The tetragonal cell (space group: $I4_1/a$) of cobalt (II) N-(2-pyrazylcarbonyl)-2-pyrazine-carboxamide, $[Co(dpzca)_2]$, adopted for the electronic structure calculations. Dark blue and light blue atoms are Co atoms and N atoms, respectively. Red sites represent O sites, and brown atoms are C atoms. H atoms are not shown in this rendition of the unit cell. The unit cell contains four molecules.

transition, as reported previously [1, 3, 4]. This thermal transition is observed in the region of 168 K and exhibits a characteristic hysteretic behavior.

The low spin state magnetic moment has been variously reported as roughly 1.9 μ_B per Co atom [3], 2.5 μ_B per Co atom [1], and 2.75 μ_B per Co atom [4], which is qualitatively in agreement with the experimental value seen here of about 1.76 μ_B per Co atom, at 130 K. It has been noted that spin crossover systems [13], including the present case of $[Co(dpzca)_2]$, have experimental values [1, 3, 4] for the magnetic moment which exceeds expectations. From density functional theory, we find lower values of the net magnetization per molecule at 2.3 μ_B per Co atom

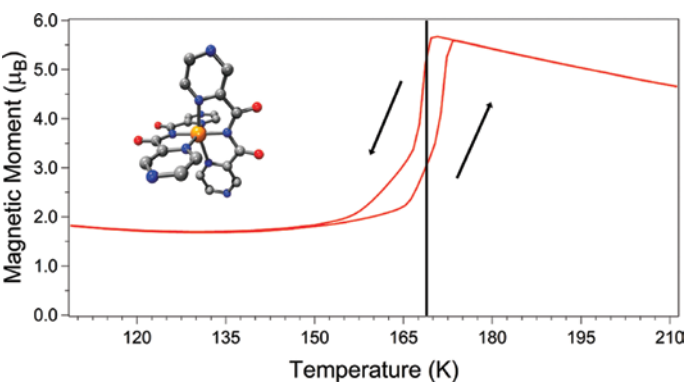

Fig. 2: The magnetic moment of $[Co(dpzca)_2]$, as a function of temperature, in the region of the spin crossover transition. The insert is a schematic of $[Co(dpzca)_2]$, taken from [3]. The region of the thermal spin crossover transition is indicated by the charges seem in proximity to the vertical line.

for the high spin state and 1 μ_B per Co atom for the low spin state. The deviation of the local moment on Co in high spin state from ideal 3 μ_B is due to the *p-d* hybridization between Co and neighbor N atoms, according to density functional theory. As indicated in Figure 3, the low spin state for the Co^{2+} cation ($3d^7$) gives a non-vanishing 1 μ_B moment since there are six 3*d* electrons in the fully filled t_{2g} states while the remaining one electron occupies one e_g orbital in one spin channel, where it remains unpaired. Thus the spin crossover transition of [Co(dpzca)$_2$] reflects a transition from a moment paramagnetic state to a higher moment paramagnetic state. The larger than expected experimentally measured magnetic moments may possibly be due to ligand contributions and cooperative

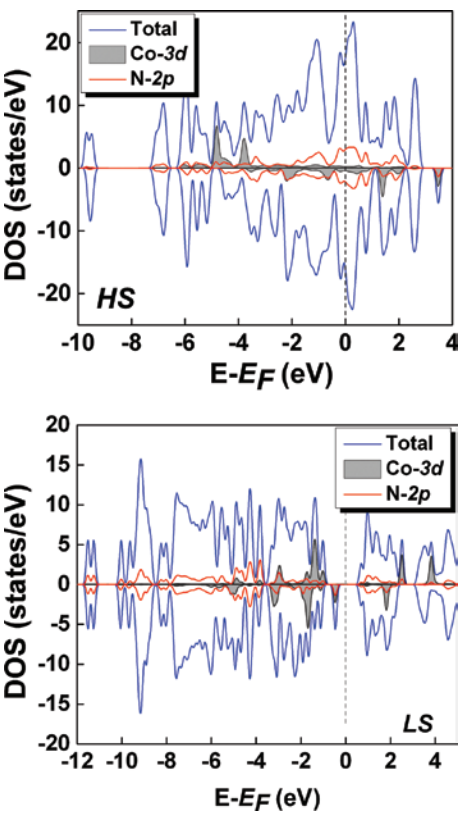

Fig. 3: The density of states for the molecule in the high spin (HS) state (resolved by spin) at top, low spin (LS) state (resolved by spin) at bottom. Blue lines corresponds to the total DOS of one molecule, the shadow area gives partial 3*d* states on Co, and the red lines depicts the contribution from N-2*p* states within the Co ligand.

effects, but key is that the low spin state moment of [Co(dpzca)$_2$] is not zero, as expected, in either experiment or theory.

Before discussing the experimental data on unoccupied electronic structure and the correspondence of this electronic structure to the magnetic moment, it is valuable to discuss the effect of the Coulomb correlation energy U on the high spin state, and low spin state energy landscapes, see Figures 4 and 5. The Coulomb correlation energy U not only splits the filled and unfilled 3d states, but also modifies the occupation number of 3d orbitals and the strength of p-d hybridization. In our calculations, the energy difference or energy splitting, between the low spin (LS) and the high spin (HS) states, changes dramatically depending on the choice of exchange correlation functional and the inclusion of the spin exchange splitting. For the low temperature structure of [Co(dpzca)$_2$], all four density functional approaches employed predict a positive energy splitting (i.e. the low spin state is the ground state), which decreases with increasing Coulomb correlation energy U. On the other hand, for the high temperature structure of [Co(dpzca)$_2$], we find that only in the density functional theory after Perdew, Burke, and Ernzerhof (PBE), with the Coulomb correlation energy U considered (i.e. PBE + U), predicts the correct negative sign of HS-LS energy difference seen, i.e. the high spin (HS) state is more stable than the low spin (LS) state when the high spin state structure is adopted. Thus a correct description of the stable spin state, based on the known structure of the high state, depends significantly on the choice of theoretical methodology. Unlike for the low temperature structure of [Co(dpzca)$_2$], for the

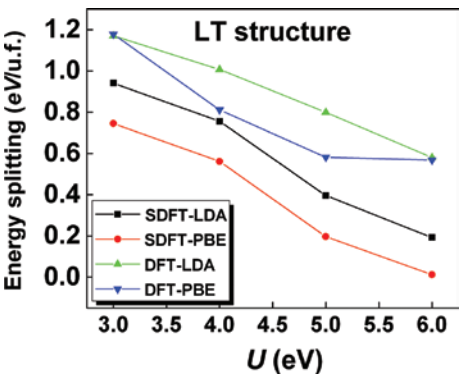

Fig. 4: The dependence of the low spin state-low spin state energy splitting as a function of the choice of Coulomb correlation energy U using various local density approximation (LDA) and Perdew, Burke, and Ernzerhof (PBE) exchange and correlation density functional theory (DFT) functionals, for the low temperature (LT) structure. SDFT corresponds to spin polarized the DFT calculation; DFT provides the normal DFT + U calculational results but with no built-in exchange parameter.

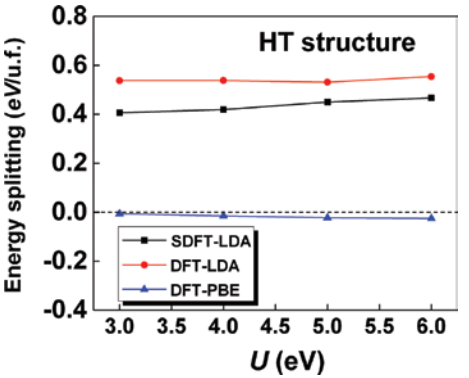

Fig. 5: The dependence of the HS-LS energy difference (or energy splitting), as a function of the choice of Coulomb correlation energy U using various local density approximation (LDA) and Perdew, Burke, and Ernzerhof (PBE) exchange correlations density functional theory (DFT) functionals, for the high temperature (HT) structure. SDFT corresponds to the spin polarized "spin" DFT calculation; again DFT provides the normal DFT + U results but with no built-in exchange parameter.

high temperature structure of [Co(dpzca)$_2$], the high spin/low spin energy difference is quite inert to the choice of Coulomb correlation energy U, even though the energy splitting is only 22 meV at $U = 5.0$ eV.

Such a strong influence of the low spin state, on the choice of Coulomb correlation energy U, while the high spin state remains relatively insensitive to the choice of U, as has been seen before in Fe II spin crossover molecular systems [5], and may be ascribed to the subtleties of the electronic structure of both structures.

4.2 The correlation of electronic structure and magnetometry

As a confirmation that the magnetometry is indeed a reflection of the electronic structure, we have compared the change in the X-ray absorption spectra (XAS) with results from magnetic susceptibility measurements. The X-ray absorption spectra (XAS) of the Co L_{III}, or $2p_{3/2}$ edge were measured as a function of temperature, as seen in Figure 6. The XAS spectra mainly result from the state transition of electrons from the $2p$ core level excited to $3d$ empty orbital. As noted above, in the low spin state of a [Co(dpzca)$_2$] spin crossover molecule, six electrons of the Co $3d$ orbital are paired up and occupy the t_{2g}-like orbital. Another single electron occupies the e_g-like orbital and remains unpaired. The presence of both t_{2g} and e_g orbitals in one spin channel, as seen in Figure 3, is a clear indication of com-

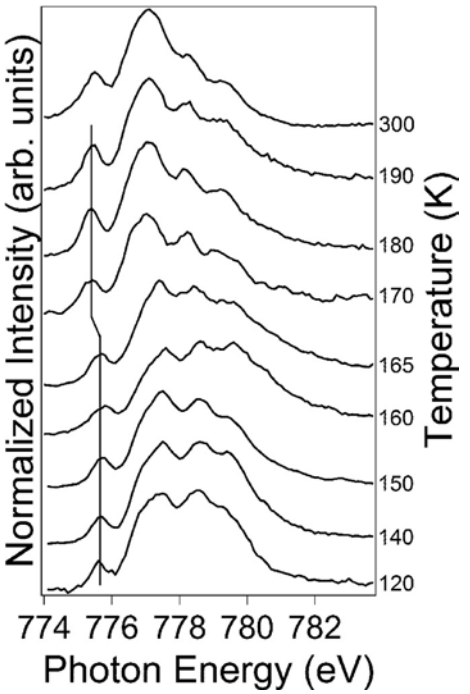

Fig. 6: The temperature-dependent X-ray absorption spectroscopy (XAS) of [Co(dpzca)$_2$]. We can assume the spectrum at 300 K is representative of the high spin state. Similarly, the spectrum at 120 K is representative of the total low spin state. The line is intended to guide the eye as to the shift in the leading absorption edge from low spin to high spin (see text).

plexity in the electronic structure of [Co(dpzca)$_2$], and is reflected in the complex Co L_{III} ($2p_{3/2}$) peak shape in the X-ray absorption spectra (XAS), as seen in Figure 6.

There are differences in the calculated [Co(dpzca)$_2$] unoccupied Co-weighted density of states (Figure 3) and the experimental XAS spectra (Figure 6). This is, in fact, expected from the changing placement of the t_{2g}-like and e_g-like empty orbitals predicted by density functional theory, as indicated by a comparison of the t_{2g}-like and e_g-like empty orbitals in the low spin (Figure 7) and high spin (Figure 8) states. There is a need for considerable caution in interpreting the XAS spectra, as an accurate assessment of the XAS spectra needs to include an assessment of all possible multiplet and final state configurations, including perturbative many-body effects, that could influence the spectra, as well as additional complications from matrix element effects. Nonetheless, theory does correctly predict the observed changes of absorption envelope of the Co 2*p* XAS spectra. The shifts in relative intensities, in the XAS absorption envelope between photon energies 777 eV and 780 eV are expected across the spin cross-over transition temperature,

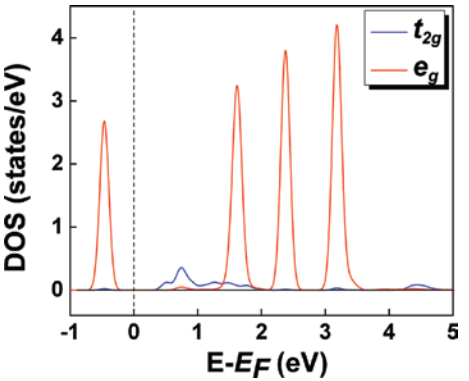

Fig. 7: The total t_{2g} state and e_g like partial density of states of [Co(dpzca)$_2$] in low spin (LS) state: only three out of four e_g orbitals are empty, two from one spin channel and the rest one from the other spin channel.

based on the DFT calculations of Figure 3. The absorption edge should be located at a higher photon energy in the low spin state, relative to the high spin state, based on the placement of the lowest unoccupied t_{2g}-like and e_g-like empty orbitals in the low spin (Figure 7) and high spin (Figure 8) states. As seen in Figure 6, there are changes in the onset energy indicative of a changing density of states in the region where the lowest unoccupied density of states resides, as indicated by Figure 3, and while this shift is only about 300 meV small, it is part of the signature of the spin cross-over transition in X-ray absorption. In fact this shift in the XAS onset is consistent with the expectations from theory (Figure 7), but remains reasonable, because the resolution in XAS is limited and this would diminish

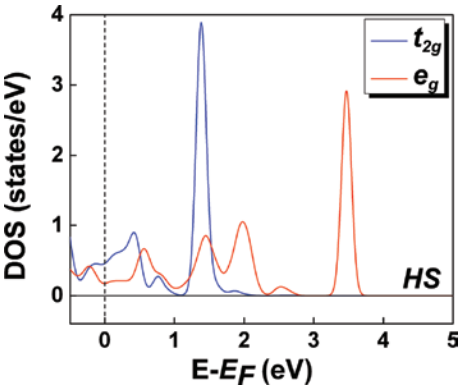

Fig. 8: The total t_{2g} state and e_g like partial density of states of [Co(dpzca)$_2$] in high spin (HS) state: two e_g orbitals and one t_{2g} are empty, all from the same spin channel.

the value of the experimentally observed shift(s). Unlike for the corresponding Fe spin crossover complexes [5], where there are profound changes in the unoccupied density of states evident in XAS, these changes are far more subtle for [Co(dpzca)$_2$], and thus more difficult to identify.

By assuming that the XAS spectrum at 300 K is representative of the high spin state and that the XAS spectrum taken at 120 K is a signature of the low spin state, we can use these two spectra as a benchmark to assess the fraction of [Co(dpzca)$_2$] in the high spin state, as a function of temperature, circumventing the deficiencies of ground state density functional theory. This estimate of the high spin state content has been plotted in Figure 9, along with the measured magnetic susceptibility, for comparison. We find the agreement between the electronic signature of the [Co(dpzca)$_2$] spin crossover transition and that of the magnetometry is quite good.

4.3 The X-ray induced excited spin state trapping of the high spin state

The best-documented method to extrinsically induce a spin crossover transition is light activation of the high spin state (light-induced excited spin-state trapping or LIESST), at temperatures well below the thermal SCO transition temperature, where the low spin state should be dominant [14–24]. Similarly soft X-ray

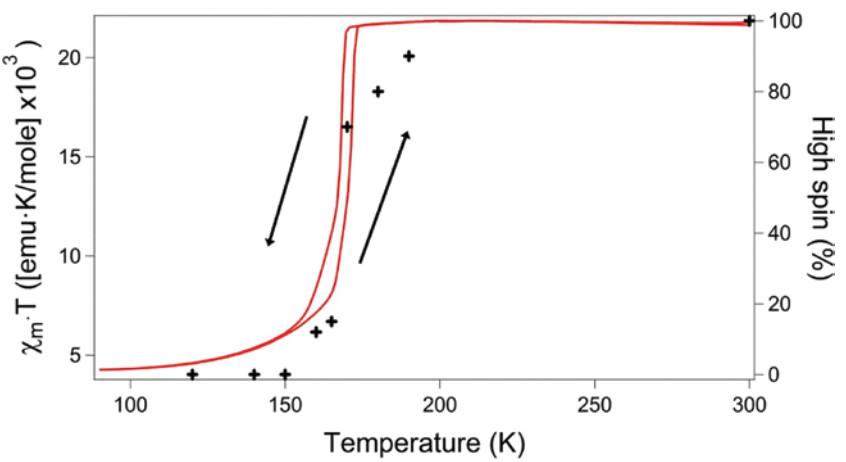

Fig. 9: The proportion of high spin state occupation derived from the temperature-dependent X-ray absorption spectroscopy (XAS) of [Co(dpzca)$_2$] (denoted by black crosses). This is compared to the magnetic susceptibility χ_mT (red line).

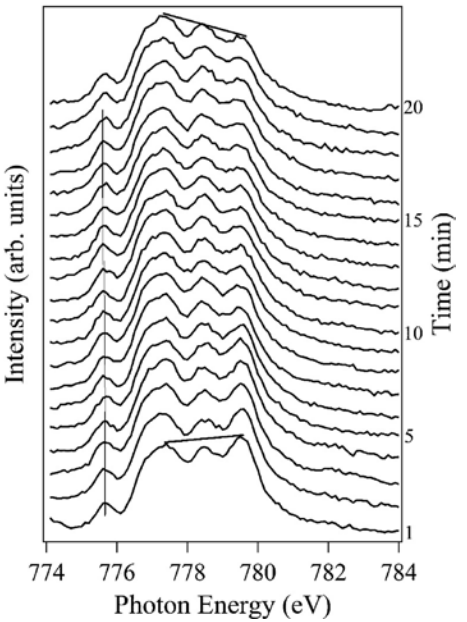

Fig. 10: The time-dependent X-ray absorption spectroscopy (XAS) of [Co(dpzca)$_2$], taken at 15 K, showing the gradual change from low spin to high spin state with continuous soft X-ray irradiation.

induced excited spin state trapping (SOXIESST) [19] and (meta)stabilization of the high spin states at low temperatures have also been reported. Both SOXIESST and LIESST require the experiments be performed at lower temperatures, in order to create a stabilized metastable light-induced high spin state that may or may not be similar to the thermodynamic, charge neutral, paramagnetic high spin state observed at high(er) temperatures. Interestingly, there is some evidence of soft X-ray induced excited state transition and trapping (SOXIESST) for [Co(dpzca)$_2$], as seen in Figure 10, where a gradual change from low spin to high spin state with continuous soft X-ray irradiation at 15 K is visible. Similar results were found over the sample temperature range of 14–18 K. Whether caused by a photoemission process or a secondary electron process cannot be discerned from the data presented here, and the experimental arrangement has not permitted assessment of the local moment soft X-ray induced excited state for [Co(dpzca)$_2$].

While by no means identical, the soft X-ray induced excited state trend in the XAS spectra of [Co(dpzca)$_2$] does somewhat resemble the evolution of the XAS spectra, for the thermal spin crossover transition in Figure 6. More explicitly, the shift in relative intensities, in the XAS absorption envelope between photon

energies 777 eV and 780 eV, seen in Figure 10, reflects the expected changes in the e_g and t_{2g} unoccupied state partial density of states, as seen in Figures 7 and 8. While there is a need for considerable caution, as an accurate assessment of the XAS spectra needs to include an assessment of all final state configurations, as noted above, theory predicts an absorption envelope should have relatively higher absorption at the leading edge (777 eV) than the trailing edge (780 eV) in the low spin state (Figure 7), while the reverse is true for the high spin state (Figure 8). Thus Figure 10 could reflect a gradual change of $[Co(dpzca)_2]$, at a constant temperature of 15 K, from a 'mostly' low spin state, to a high spin state, under X-ray fluence. It must be acknowledged that there is no reason that the latter is a Co II charge neutral state, and confirmation of this soft X-ray induced excited state moment remains outstanding.

This soft X-ray induced excited state is observed to relax back to the low spin state after about 5 h, at 19 K, in the absence of further X-ray irradiation. The molecule could be repeatedly excited again, by soft X-rays, as in Figure 10, after relaxing back into low spin state. This excludes the possibility of molecule damage due to the X-ray irradiation. There is a shift in the onset Co $2p_{3/2}$ absorption edge energy, and while this shift is smaller than seen in Figure 6, this and the increase in the intensity of the absorption peak at roughly 777.4 eV photon energy and the shift of this feature to lower photon energies with increasing X-ray exposure are parts of the signature of the spin cross-over transition in X-ray absorption. At the very least, the existence of reversible soft X-ray induced excited state trapping is consistent with the reversible redox reactions seen for $[Co(dpzca)_2]$ [2, 3].

The distinct SOXIESST electronic excited states may include singlet and triplet states as well as metal-to-ligand charge transfer states [15–17, 25–30]. The fact that there are clear similarities between the time evolution of the XAS spectra as part of the soft X-ray induced excited state transition of Figure 10 and the evolution of the XAS spectra with temperature, across the thermal spin crossover transition (Figure 6), does suggest that the high spin state of $[Co(dpzca)_2]$, seen above 170 K is related to a SOXIESST high spin electronic excited state. Valence tautomeric spin crossover transitions may occur in the thermal spin crossover transition, as well as in the light-induced excited spin-state trapping or LIESST transition at low temperatures, as seen in the $[\{Co^{III\text{-}LS}(tpa)\}_2(dhbq^{3-})]^{3+} \Leftrightarrow [Co^{III\text{-}LS}(tpa)(dhbq^{2-})Co^{II\text{-}HS}(tpa)]^{3+}$ transition [16, 31].

The very short lifetime SOXIESST electronic excited states have been observed for some spin crossover molecular systems, in aqueous solution at room temperature [25, 28]. Given the stability $[Co(dpzca)_2]$ [2, 3], this too seems like a likely candidate for such experiments.

5 Conclusions

In summary, we have investigated the electronic structure of [Co(dpzca)$_2$] with symmetric pyrazine imide ligands, at various temperatures. Our calculations demonstrate that the choice of Coulomb repulsion energy is seen to have a more profound effect on the calculated electronic structure of the low spin state, but little influence on the electronic structure of the high spin state. Our XAS measurements as a function of X-ray exposure, show spectroscopic similarities to the thermal spin crossover transition. This is indicative of an X-ray induced excited spin state trapping for [Co(dpzca)$_2$] at 15 K. Specifically the X-ray induced excited state at 15 K resembles the high spin state of [Co(dpzca)$_2$] obtained thermally by increasing temperature to above 175 K.

Acknowledgments: This research was supported by the National Science Foundation through the Nebraska MRSEC (DMR-1420645) and through the Division of Chemistry and Division of Materials Research (NSF-1565692). Partial financial support of the Nebraska Center for Energy Sciences Research (cycle 11) is also gratefully acknowledged. The Advanced Light Source is supported by the Director, Office of Science, Office of Basic Energy Sciences, of the U.S. Department of Energy under Contract No. DE-AC02-05CH11231.

References

1. R. G. Miller, S. Narayanaswamy, J. L. Tallon, S. Brooker, New J. Chem. **38** (2014) 1932.
2. M. G. Cowan, R. G. Miller, S. Brooker, Dalton Trans. **44** (2015) 2880.
3. M. G. Cowan, J. Olguín, S. Narayanaswamy, J. L. Tallon, S. Brooker, J. Am. Chem. Soc. **134** (2012) 2892.
4. R. G. Miller, S. Narayanaswamy, S. M. Clark, P. Dera, G. B. Jameson, J. L. Tallon, S. Brooker, Dalton Trans. **44** (2015) 20843.
5. X. Zhang, S. Mu, G. Chastanet, N. Daro, T. Palamarciuc, P. Rosa, J.-F. Létard, J. Liu, G. E. Sterbinsky, D. A. Arena, C. Etrillard, B. Kundys, B. Doudin, P. A. Dowben, J. Phys. Chem. C **119** (2015) 16293.
6. P. Nachimuthu, J. H. Underwood, C. D. Kemp, E. M. Gullikson, D. W. Lindle, D. K. Shuh, R. C. C. Perera, in: AIP Conf. Proc., AIP Publishing, (2004), P. 454.
7. P. E. Blöchl, Phys. Rev. B **50** (1994) 17953.
8. G. Kresse, J. Hafner, Phys. Rev. B **48** (1993) 13115.
9. G. Kresse, J. Furthmüller, Phys. Rev. B **54** (1996) 11169.
10. A. I. Liechtenstein, V. I. Anisimov, J. Zaanen, Phys. Rev. B **52** (1995) R5467.
11. J. P. Perdew, K. Burke, M. Ernzerhof, Phys. Rev. Lett. **77** (1996) 3865.
12. J. Chen, A. J. Millis, C. A. Marianetti, Phys. Rev. B **91** (2015) 241111.

13. X. Zhang, T. Palamarciuc, J.-F. Létard, P. Rosa, E. V. Lozada, F. Torres, L. G. Rosa, B. Doudin, P. A. Dowben, Chem. Commun. **50** (2014) 2255.
14. J.-F. Létard, P. Guionneau, L. Goux-Capes, Towards Spin Crossover Applications, in: P. Gütlich, H. A. Goodwin (Eds.): Spin Crossover Transit. Met. Compd. III, Springer, Berlin Heidelberg (2004), P. 221–249.
15. P. Gütlich, H. A. Goodwin, in: P. Gütlich, H. A. Goodwin (Eds.): Spin Crossover Transit. Met. Compd. I, Springer Berlin Heidelberg (2004), P. 1–47.
16. O. Sato, J. Tao, Y.-Z. Zhang, Angew. Chem. Int. Ed. **46** (2007) 2152.
17. J. A. Real, A. B. Gaspar, M. C. Muñoz, Dalton Trans. (2005) 2062.
18. J.-J. Lee, H. Sheu, C.-R. Lee, J.-M. Chen, J.-F. Lee, C.-C. Wang, C.-H. Huang, Y. Wang, J. Am. Chem. Soc. **122** (2000) 5742.
19. B. Warner, J. C. Oberg, T. G. Gill, F. El Hallak, C. F. Hirjibehedin, M. Serri, S. Heutz, M.-A. Arrio, P. Sainctavit, M. Mannini, G. Poneti, R. Sessoli, P. Rosa, J. Phys. Chem. Lett. **4** (2013) 1546.
20. T. G. Gopakumar, M. Bernien, H. Naggert, F. Matino, C. F. Hermanns, A. Bannwarth, S. Mühlenberend, A. Krüger, D. Krüger, F. Nickel, W. Walter, R. Berndt, W. Kuch, F. Tuczek, Chem. – Eur. J. **19** (2013) 15702.
21. J.-F. Létard, G. Chastanet, P. Guionneau, C. Desplanches, Optimizing the Stability of Trapped Metastable Spin States, in: L. a Halcrow (Ed.): Spin-Crossover Mater., John Wiley & Sons Ltd, New York (2013), P. 475–506.
22. M. Marchivie, P. Guionneau, J. A. K. Howard, G. Chastanet, J.-F. Létard, A. E. Goeta, D. Chasseau, J. Am. Chem. Soc. **124** (2002) 194.
23. L. Capes, J.-F. Létard, O. Kahn, Chem. – Eur. J. **6** (2000) 2246.
24. N. Moliner, L. Salmon, L. Capes, M. C. Muñoz, J.-F. Létard, A. Bousseksou, J.-P. Tuchagues, J. J. McGarvey, A. C. Dennis, M. Castro, R. Burriel, J. A. Real, J. Phys. Chem. B **106** (2002) 4276.
25. W. Zhang, R. Alonso-Mori, U. Bergmann, C. Bressler, M. Chollet, A. Galler, W. Gawelda, R. G. Hadt, R. W. Hartsock, T. Kroll, K. S. Kjær, K. Kubiček, H. T. Lemke, H. W. Liang, D. A. Meyer, M. M. Nielsen, C. Purser, J. S. Robinson, E. I. Solomon, Z. Sun, D. Sokaras, T. B. van Driel, G. Vankó, T.-C. Weng, D. Zhu, K. J. Gaffney, Nature **509** (2014) 345.
26. C. Creutz, M. Chou, T. L. Netzel, M. Okumura, N. Sutin, J. Am. Chem. Soc. **102** (1980) 1309.
27. N. Huse, H. Cho, K. Hong, L. Jamula, F. M. F. de Groot, T. K. Kim, J. K. McCusker, R. W. Schoenlein, J. Phys. Chem. Lett. **2** (2011) 880.
28. H. T. Lemke, C. Bressler, L. X. Chen, D. M. Fritz, K. J. Gaffney, A. Galler, W. Gawelda, K. Haldrup, R. W. Hartsock, H. Ihee, J. Kim, K. H. Kim, J. H. Lee, M. M. Nielsen, A. B. Stickrath, W. Zhang, D. Zhu, M. Cammarata, J. Phys. Chem. A **117** (2013) 735.
29. W. Zhang, K. S. Kjær, R. Alonso-Mori, U. Bergmann, M. Chollet, L. A. Fredin, R. G. Hadt, R. W. Hartsock, T. Harlang, T. Kroll, K. Kubiček, H. T. Lemke, H. W. Liang, Y. Liu, M. M. Nielsen, P. Persson, J. S. Robinson, E. I. Solomon, Z. Sun, D. Sokaras, T. B. van Driel, T.-C. Weng, D. Zhu, K. Wärnmark, V. Sundström, K. J. Gaffney, Chem. Sci. **8** (2016) 515.
30. T. Tezgerevska, K. G. Alley, C. Boskovic, Coord. Chem. Rev. **268** (2014) 23.
31. J. Tao, H. Maruyama, O. Sato, J. Am. Chem. Soc. **128** (2006) 1790.